Available online at www.sciencedirect.com
SCIENCE DIRECT
Polymer 46 (2005) 3289–3299
polymer
www.elsevier.com/locate/polymer

# Composites of allyl glycidyl ether modified polyethylene and cellulose

R. Casarano[a], J.R. Matos[a], M.C.A. Fantini[b], D.F.S. Petri[a,*]

[a]*Instituto de Química, Universidade de São Paulo, P.O. Box 26077-05599-970 São Paulo, Brazil*
[b]*Instituto de Física, Universidade de São Paulo, São Paulo, Brazil*

Received 21 September 2004; received in revised form 4 February 2005; accepted 22 February 2005
Available online 24 March 2005

**Abstract**

Linear medium density polyethylene (LMDPE) was functionalized with allyl glycidyl ether (AGE) in an internal laboratory mixer in the presence of peroxide. AGE is a bifunctional monomer, which forms unstable and energetically rich macroradicals. Upon increasing the peroxide content chain scission and grafting yield were favored. The degree of functionalization was determined by means of a calibration function for Fourier-transformed infrared spectroscopy (FTIR). Grafting AGE onto LMDPE led to a small loss of crystallinity, as evidenced by differential scanning calorimetry (DSC) and X-ray diffractometry analyses. Composites of LMDPE or functionalized LMDPE-AGE and cellulose were prepared in the mixer with filler contents ranging from 20 to 50 wt%. Composites of AGE functionalized LMDPE and filler content higher than 30 wt% presented tensile properties superior to that observed for composites with unmodified LMDPE. Scanning electron microscopy (SEM) on the composites fracture surface evidenced good interfacial adhesion between LMDPE-AGE and cellulose fibers.


*Keywords:* Polyethylene; Allyl glycidyl ether; Cellulose

## 1. Introduction

Many efforts have been devoted to the development of composites of thermoplastics and natural fibers. Weight reduction, low cost, environmental benefits are some of the advantages offered by natural fibers reinforced materials, which are solid dispersions. The mechanical performance of such dispersions depends strongly on the interfacial adhesion between dispersed phase and matrix. Since both phases are immiscible, at least one of the phases must be modified with functional groups, which are capable to form chemical bonds with the other phase. The functionalization reaction can occur either on the surface [1,2] or in the bulk [1]. The choice of a functional group is made with basis on its reactivity and its affinity for the other phase. For instance, composites of maleated polyolefins and cellulose have been extensively studied [1,3–10]. Grafting maleic anhydride (MA) onto the polyolefins increases the compatibility through the esterification between the MA groups and the hydroxyl groups of cellulose [8–11]. Other polar functional groups like tetrahydrophthalic anhydride [12] and glycidyl methacrylate [13–20] proved to be advantageous. Allyl glycidyl ether (AGE) is a bifunctional molecule with a terminal epoxy and a terminal allyl groups. AGE has been largely used to modify cellulose [21–26], by the reaction of AGE epoxy group with the cellulose hydroxyl groups. The modified cellulose chains carry vinyl groups, which can easily react in the presence of the proper initiator. However, grafting AGE onto polymer chains by the addition reaction to the allyl group has been seldom reported. AGE is an interesting monomer because it forms unstable and energetically rich macroradicals.

This work focuses on the AGE grafting reaction onto linear medium density polyethylene (LMDPE) in the melt in the presence of benzoyl peroxide (BPO), as initiator. Composites of functionalized LMDPE-AGE and cellulose fibers were prepared with different filler contents. The interfacial adhesion between polymeric matrix and filler was evaluated by means of tensile test and scanning electron microscopy.

* Corresponding author. Tel.: +55 11 3091 3831; fax: +55 11 3815 557.
*E-mail address:* dfsp@iq.usp.br (D.F.S. Petri).

0032-3861/$ - see front matter © 2005 Elsevier Ltd. All rights reserved.
doi:10.1016/j.polymer.2005.02.077

Table 1
Formulations used in the internal laboratory mixer

| Sample | LMDPE (g) | BPO (g) | AGE (g) | $\tau_f$ (Nm) | DF (wt% of AGE) | MFI [g((10 min)] |
|---|---|---|---|---|---|---|
| LMDPE | 40 | – | – | 15.0±0.5 | – | 1.7 |
| LMDPE-BPO | 40 | 1.70 | – | 16.5±0.5 | – | 0.3 |
| LMDPE-AGE-1 | 45 | 1.90 | 9.0 | 2±1 | 0.74 | 0.2 |
| LMDPE-AGE-2 | 45 | 0.63 | 9.0 | 13.6±0.7 | 0.28 | 0.3 |

Control and LMDPE functionalization experiments. $\tau_f$ represents the torque values at the end of the process. DF is the degree of functionalization determined from the calibration curve (see text for more details).

## 2. Experimental section

### 2.1. Materials

Linear medium density poly(ethylene-*co*-butene) (LMDPE) with melt flow index of 1.7 g/(10 min) and density of 0.932 g/cm$^3$ was kindly supplied by Politeno (Brazil). Benzoyl peroxide (BPO, molecular weight = 242.23 g/mol) from Vetec, Brazil, and allyl glycidyl ether (AGE, molecular weight = 114.14 g/mol, A32608, Aldrich, Germany, $T_b$ = 154 °C) were used without further purification. Short cellulose (SC) fibers were purchased from Fluka (9004-34-6, Switzerland). The fibers mean diameter and length (0.030±0.008 and 0.13±0.07 mm, respectively) were measured using a Carl Zeiss Axioplan 2 optical microscope equipped with a Leica Q550 IW image analyzer software.

### 2.2. Methods

#### 2.2.1. Reactive processing and compounding

LMDPE was molten in an internal laboratory mixer Haake Polylab R600—Thermo Electron (Karlsruhe) GmbH at 120 °C and 60 rpm during 6 or 7 min. After 3 or 4 min, AGE and BPO were added together to the melt to limit the risks of AGE evaporation or advanced decomposition of BPO. The exactly quantities of each reactant are listed in Table 1. The functionalized LMDPE-AGE samples were removed and cut into small pellets without any purifying process. In a second processing step, LMDPE-AGE was molten at 150 °C and 80 rpm during 5 min and then cellulose fibers were added, mixing during additional 30 min. The cellulose content varied from 20 to 50 wt%. The SC fibers were vacuum dried at 70 °C for 10 days before compounding with the polyolefins. The composites prepared with functionalized LMDPE-AGE samples were coded as LMDPE-AGE-SC. In order to verify the compatibilizing effect of AGE, control composites were prepared in the absence of AGE by the same methods and coded as LMDPE-SC. After the compounding, the composites were taken out and shaped into small pellets. All processes were carried out without mixer degassing or $N_2$ purging.

#### 2.2.2. Sheet preparation

Sheets of LMDPE, LMDPE-BPO, LMDPE-AGE-1, LMDPE-AGE-2 and composites were prepared by a compression-molding method. The pellets were pressed at 170 °C and 150 kgf/cm$^2$ for 10 min using a Sirma pneumatic press. The sheet thickness was adjusted by using a metal frame 1.6 mm thick.

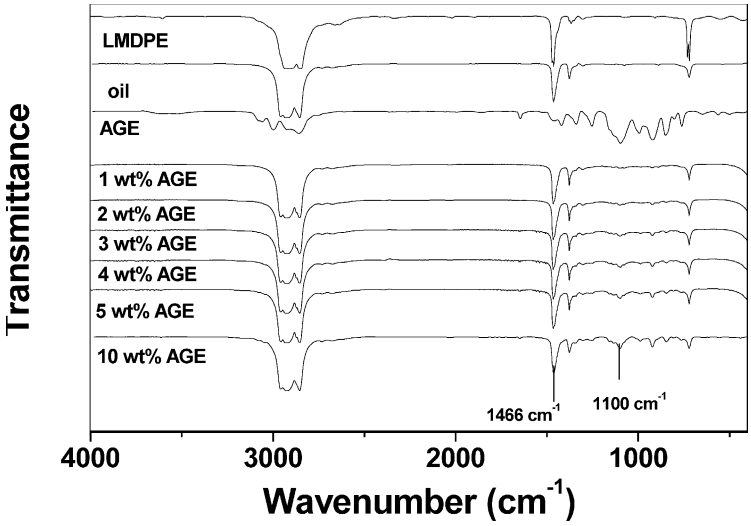


Fig. 1. FTIR spectra obtained for LMDPE, AGE, mineral oil, and mixtures of AGE and mineral oil.

*2.2.3. Determination of the degree of functionalization by FTIR vibrational spectroscopy*

Fourier transform infrared (FTIR) spectra were obtained in a Bomem© MB100 equipment with the resolution of 4 $cm^{-1}$ and 32 scans per spectrum. Prior to the FTIR analyses, the functionalized LMDPE-AGE samples were purified by dissolution in toluene at 110 °C and then precipitated in acetone at room temperature. The precipitated samples were filtered and dried in the air. Finally the precipitate was rinsed in acetone in a Soxhlet extractor during 16 h. This purification process allows to remove the non-reacted initiator, non-reacted AGE and oligomers or homopolymers of AGE. The samples were dried in vacuum at 100 °C during 24 h prior to the characterization. The polymeric films were prepared by casting hot polymer solutions in toluene at the concentration of 10.0 g/L.

The degree of functionalization (DF) was determined with basis on a calibration curve made from mixtures of a mineral oil and AGE. This was possible because the mineral oil and LMDPE show similar spectra (Fig. 1). Fig. 1 shows the spectra of LMDPE, AGE, mineral oil and mixtures of AGE and mineral oil with 1, 2, 3, 4, 5 and 10 wt% of AGE. For calibration curve the characteristic band of $CH_2$ (scissoring) at 1466 $cm^{-1}$ present in the mineral oil and in LMDPE spectra and the AGE characteristic band at 1100 $cm^{-1}$, assigned to the asymmetric stretching vibration of the C–O–C, were chosen. The ratio between the intensity corresponding to the epoxy characteristic band at 1100 $cm^{-1}$, $I_{1110}$, and the intensity corresponding to the characteristic band of $CH_2$ (scissoring) at 1466 $cm^{-1}$, $I_{1466}$, increased with the AGE content (wt%) in the mixture, as shown in Fig. 2. The variation of $I_{1100}/I_{1466}$ with AGE content could be fitted with the polynomial equation $y = 0.039 + 0.050\,x - 0.002\,x^2$, and $R = 0.99747$. Therefore, the DF, expressed as wt% of AGE, was estimated by substituting the ratio $I_{1100}/I_{1466}$ measured for the functionalized LMDPE samples in this polynomial equation. The determination of grafting yield by means of FTIR calibration curves is commonly reported [14,15,27].

The grafting yield of AGE onto LMDPE was not determined by elementary analysis of oxygen because the obtained values reached the limit of the sensitivity of the measuring equipment.

X-ray diffractometry (XRD) experiments were performed in a Rigaku diffractometer, Bragg-Brentano geometry, using monochromatized $CuK_\alpha$ radiation ($\lambda = 0.154$ nm), at 40 kV and 20 mA. Wide angle X-ray intensities (WAXS) were collected from $2\theta$ range of 10–50° with step scanning mode of 0.05° and time intervals of 10 s. The purified samples were approximately 0.5 mm thick films, prepared by casting hot polymeric solutions on glass slides. The films were previously annealed at 120 °C under vacuum overnight.

Differential scanning calorimetry (DSC) curves were obtained in a DSC-50 cell (Shimadzu) using Al crucibles with about 2.3 mg of samples, under dynamic $N_2$ atmosphere (100 mL $min^{-1}$) and heating rate of 5 °C $min^{-1}$ in the temperature range from 25 to 150 °C. After heating the purified samples were let to cool spontaneously up to 25 °C and soon after the samples were reheated in the same conditions. The second heating was considered for the determination of $T_m$ and $\Delta H_{fus}$. The DSC cell was calibrated with In (mp 156.6 °C; $\Delta H_{fus} = 28.59$ J $g^{-1}$) and Zn (mp 419.6 °C; $\Delta H_{fus} = 111.40$ J $g^{-1}$).

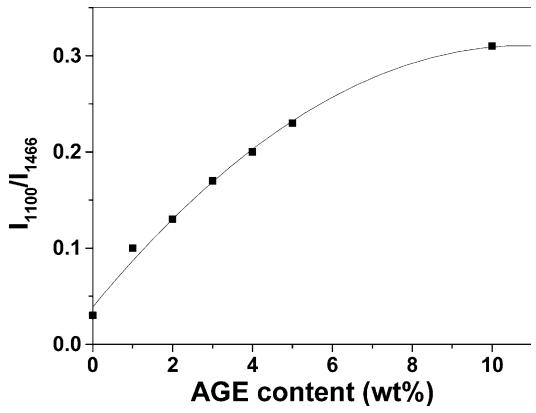


Fig. 2. Variation of $I_{1100}/I_{1466}$ with AGE content used for estimating the degree of functionalization.

Melt flow indices were determined for LMDPE and purified LMDPE-AGE samples in a Kayeness Galaxy I Melt Indexer following the test method by ASTM D1238 (190 °C and 2.16 kg).

Tensile tests were performed for composites and original LMDPE samples according to the standard testing method ASTM D638-95. The tensile properties were determined for five samples of same composition in an INSTRON 4400R equipment at room temperature.

Scanning Electron Microscopy (SEM) analyses on the composites crio-fracture surfaces were obtained in a Phillips XL30 equipment. In order to avoid artifacts due to plastic deformations the samples were fractured under liquid $N_2$. The surfaces were coated with a thin (~30 nm) layer of sputtered gold prior to the analysis.

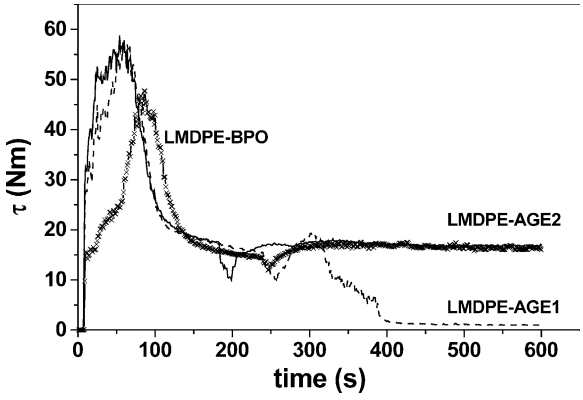


Fig. 3. Torque as a function of time obtained for LMDPE-BPO (line and symbol), LMDPE-AGE-1 (dotted line) and LMDPE-AGE-2 (solid line).

## 3. Results and discussion

### 3.1. Grafting AGE onto LMDPE

The functionalization of LMDPE samples in the internal laboratory mixer followed the formulations presented in Table 1. LMDPE and LMDPE-BPO are control experiments and allow estimating the shear effect in the absence and in the presence of BPO on the polymer. Fig. 3 shows the torque as a function of time obtained for LMDPE-BPO, LMDPE-AGE-1 and LMDPE-AGE-2. The torque values at the end ($\tau_f$) of the process found for the control experiments LMDPE (torque curve not shown) and LMDPE-BPO amounted to 15.0 and 16.5 Nm, respectively. Upon adding AGE to the mixture, the $\tau_f$ values at the end of the process varied strongly with the BPO content. The amounts of BPO in the LMDPE-AGE-1 and LMDPE-BPO samples are very similar, indicating that the combination of high amount of BPO and AGE leads to chain scission, which causes the low $\tau_f$ values. Since AGE is liquid at room temperature, the viscosity inside the mixing chamber is reduced, and therefore, the diffusion of free radicals primarily formed from BPO is faster, favoring chain scission, especially if the BPO concentration is high. The reactions, which might take place in the melt during the mixing, are schematically depicted in Scheme 1. Reaction 11 in Scheme 1 represents the polyolefin chain scission. Liu and co-workers [13] observed chain scission upon grafting glycidyl methacrylate (GMA) onto polypropylene (PP) in a similar mixer. The reduction in the PP molecular weight was evidenced by an increase in the MFI. Bettini and Agnelli [28] showed that upon grafting maleic anhydride onto PP by reactive processing, the increase in the BPO content led to an increase in the MFI, indicating chain scission. In the present study, the MFI value determined for LMDPE-AGE-1 samples surprisingly decreased to 0.2 g/(10 min). Fig. 4 shows FTIR spectra of purified LMDPE-AGE-1 samples before and after MFI tests. The characteristic bands of LMDPE and AGE are present in both spectra. However, a band at 1720 $cm^{-1}$, characteristic of carbonyl group is present before and after MFI test with similar intensities. Although an increase in the MFI value was expected because of the low $\tau_f$ values, the LMDPE-AGE-1 samples presented very low MFI. This interesting finding might be explained by means of favorable interaction as H bonding between the AGE monomers grafted onto different LMDPE chains and carbonyl groups generated during the reactive processing by oxidation, which could cause an apparent increase in the mean molecular weight [29]. Fig. 4 also shows that the spectrum obtained for purified LMDPE-AGE-2 samples the band corresponding to the carbonyl group is very weak, indicating that the amount of BPO might also control the chains oxidation. LMDPE-AGE-2 samples presented MFI of 0.3 g/(10 min), which is similar to those found for LMDPE-BPO and LMDPE-AGE-1 (Table 1). This finding indicates that the apparent increase in the mean molecular weight due to specific interactions [29] might take place even when the amount of carbonyl group is low.

The intensity of the band at 1100 $cm^{-1}$, assigned to the asymmetric stretching vibration of the C–O–C (AGE aliphatic ether), obtained for LMDPE-AGE-2 is weaker than that observed for the LMDPE-AGE-1 samples (Fig. 4). The DF estimated from these spectra and the calibration curve (Fig. 2) amounted to 0.74 and 0.28 wt% of AGE, for LMDPE-AGE-1 and LMDPE-AGE-2, respectively. The higher the BPO concentration, the larger will be the amount of primary radicals formed and, consequently, the higher the concentration of macroradicals available for the reaction with AGE. Therefore, the higher will be the degree of functionalization. Reaction 1 in Scheme 1 represents the thermal decomposition of BPO with the production of two primary radicals ($I^{\cdot}$). In the proposed mechanism these radicals abstract H atoms from the LMDPE chains, forming macroradicals (reaction. 2). The addition of the macroradical to the AGE double bond (reaction 3) and further H transfer reaction (reaction 4) lead to the functionalized LMDPE-AGE, which is the desired product (LMDPE-AGEa). Reactions combining the macroradical and the AGE radical (reactions 5 and 6) also yield LMDPE-AGEb and LMDPE-AGEc. One should notice that the products resulting from reactions 4–6 present the epoxy group free to interact with the hydroxyl groups of polysaccharides. The homopolymerization of AGE radical forming a side chain of LMDPE (reactions 7 and 8) is also possible, yielding LMDPE-AGEd. However, a large amount of AGE would be consumed by polyolefin chain, so that only few terminal epoxy groups would be available for the interaction with the polysaccharides. Reactions involving exclusively the macroradicals as combination (reaction 9), disproportioning (reaction 10) or β-scission (reaction 11) are possible, but undesired. After grafting AGE onto LMDPE, the samples were completely soluble in xylene at 110 °C, so that reaction 9 hardly occurs during the reactive processing. In contrast, reaction 11 is an explanation for the low $\tau_f$ values after the functionalization of LMDPE-AGE-1. Increasing the peroxide concentration the grafting yield of AGE increased and the chain scission and oxidation was favored. Sun and co-workers [30] observed a similar effect upon grafting GMA onto PP in a mixer or in a co-rotating twin screw extruder [17]. Bettini and Agnelli [28] also observed that increasing the peroxide concentration the grafting yield of maleic anhydride onto PP and the MFI both increased. The general behavior is explained by the increase in the concentration of macroradicals when the peroxide concentration is enhanced. The reactions presented in Scheme 1 refer mainly to those involving the radical formation on tertiary carbons. However, the radical formation on secondary carbons is also possible.

Allyl glycidyl ether (AGE) is an interesting monomer because of its epoxy and allylic functionalities. The copolymerization parameters $Q$ and $e$ for AGE amount to

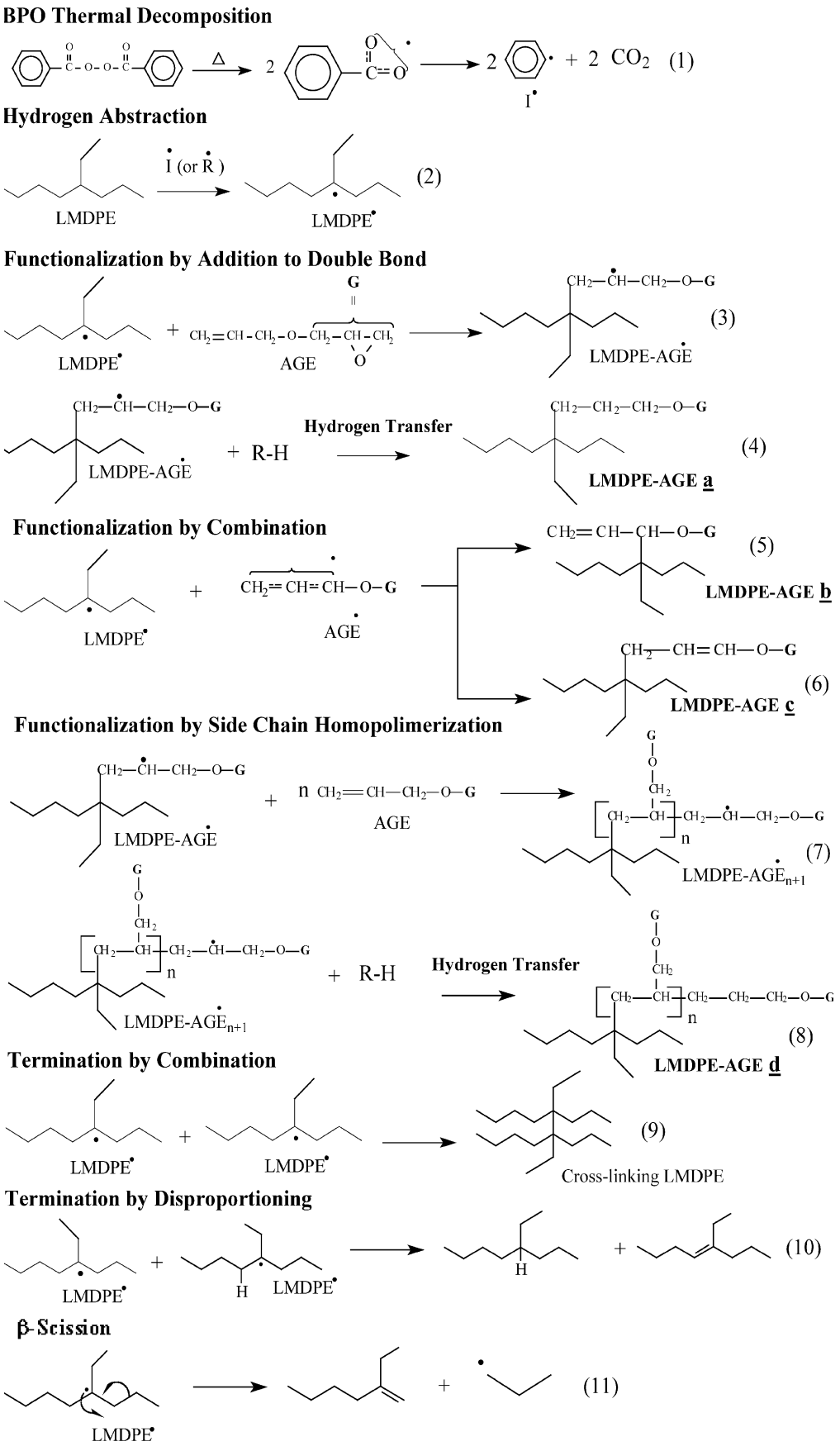


Scheme 1. Representation of free radicals formed during the reactive processing and the possible reactions (details in the text).

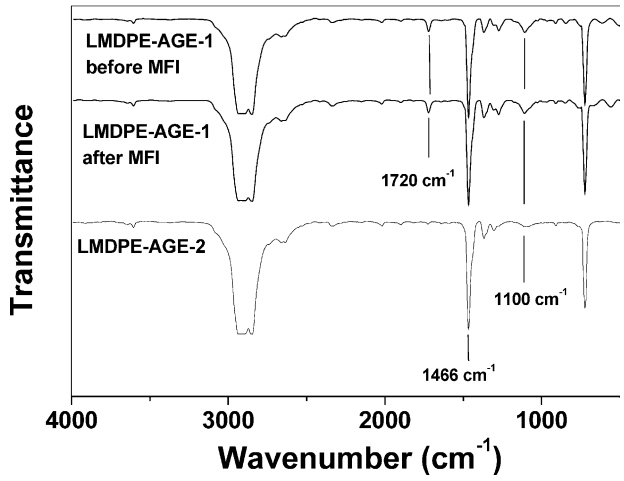


Fig. 4. FTIR spectra obtained for purified LMDPE-AGE-1 before and after MFI tests and for purified LMDPE-AGE-2 samples.

0.068 and 0.80, respectively [31]. $Q$ is a measure for the monomer reactivity, in other words, the monomer readiness to form the macroradical, in this particular case, LMDPE-AGE$^{\cdot}$ (reaction 3 in Scheme 1). If the macroradical is stabilized by resonance effect, then the radical formation will be favored. The $e$ parameter is related to the monomer polarity. Positive value indicates electron acceptor effect, negative value indicates electron donor effect. The $e$–$Q$ diagram is currently applied in copolymerization process [32] and helps to predict the structure of resulting copolymer (alternated or statistical). Styrene has been considered as a reference monomer, it presents $Q=1.0$ and $e=-0.8$ [32]. When the $e$–$Q$ values lie in the left side of the diagram, ($Q<0.1$) the macroradicals are unstable and energetically rich. That is the case for AGE, vinyl ether and allyl acetate. The macroradicals of such monomers strive to form new radicals with higher resonance stabilization either by reacting with a different monomer or by chain transfer with the same monomer. Therefore, the tendency towards polymerization of allylic compounds is rather low, indicating that reactions 7 and 8 in Scheme 1 probably do not take place. This discussion would also explain the low degree of functionalization obtained for LMDPE-AGE-1 (0.74 wt%) and LMDPE-AGE-2 (0.28 wt%). Similar grafting yield has been observed for glycidyl methacrylate (GMA) grafted onto polyolefins [15]. However, adding to the system (GMA onto polyolefins) an electron-donating monomer, as styrene, the grafting yield increased significantly [15,17]. This trick has also been applied to improve the grafting yield of maleic anhydride (MA) onto polyolefins. The $Q$ and $e$ values for MA are 0.23 and 2.25 [32], respectively, indicating that the corresponding macroradicals present higher resonance stabilization than AGE. Moreover, the electron transfer from donor to acceptor permits the creation of a charge transfer complex [15] with superior reactivity to that of free monomers, favoring the grafting reaction.

The functionalization of LMDPE with AGE was also evidenced by DSC. Typical DSC curves obtained for pure LMDPE, LMDPE-BPO, functionalized LMDPE-AGE-1 and LMDPE-AGE-2 are shown in Fig. 5. Their melt temperature ($T_m$) values determined at the peak and melt enthalpy ($\Delta H_m$) are presented in Table 2. The degree of crystallinity (DC) was calculated considering the $\Delta H_m$ value of 293 J(g reported for a 100% crystalline polyethylene sample [33]. The $T_m$ values found for LMDPE, LMDPE-BPO and LMDPE-AGE-2 samples were similar and 1.4 °C higher than that found for LMDPE-AGE-1. The $\Delta H_m$ value found for LMDPE samples is higher than those

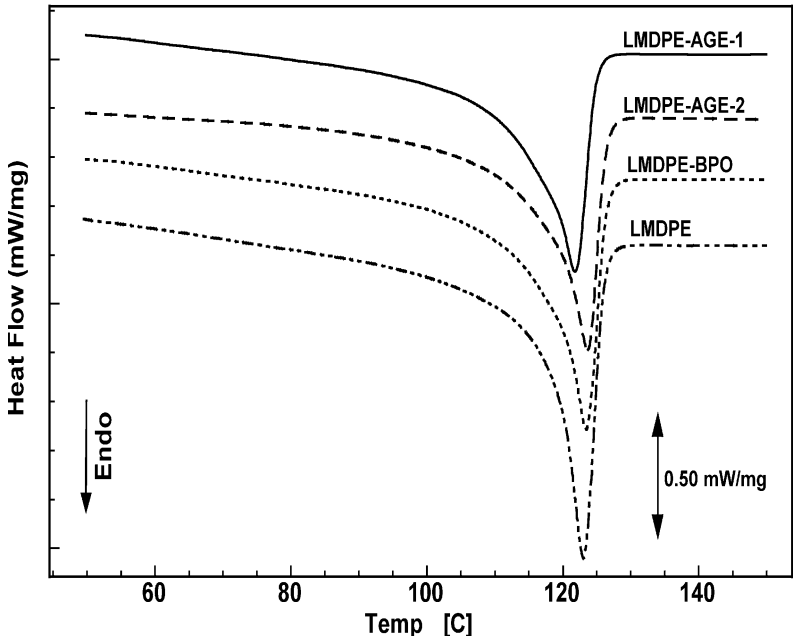


Fig. 5. DSC curves obtained for LMDPE, LMDPE-BPO, LMDPE-AGE-1 and LMDPE-AGE-2.

Table 2
Melt temperature at the peak $T_m$ (°C), melt enthalpy $\Delta H_m$ calculated in the temperature range from 80 to 140 °C and degree of crystallinity (DC)

| Sample | $T_m$ (°C) | $\Delta H_m$ (J(g) | DC (%) |
|---|---|---|---|
| LMDPE | 123.0 | 155 | 52.9 |
| LMDPE-BPO | 123.4 | 143 | 48.8 |
| LMDPE-AGE-1 | 121.8 | 128 | 43.7 |
| LMDPE-AGE-2 | 123.6 | 133 | 45.4 |

determined for LMDPE-BPO, LMDPE-AGE-1 and LMDPE-AGE-2. The corresponding DC values indicate that processing LMDPE in the presence of BPO and air might cause some chain packing perturbation, which leads to a small decrease in the sample crystallinity. AGE modified LMDPE samples with DF of 0.28 and 0.74 wt% of AGE led to the reduction in the DC of 7 and 9%, respectively.

Diffraction peaks and amorphous halo are typical features of semi-crystalline polymers. Poly(ethylene) crystallizes in the all-trans conformation and belongs to the orthorhombic crystal class. The corresponding lattice constants [34] amounts to $a=0.742$ nm, $b=0.495$ nm and $c=0.254$ nm. All WAXS diffractograms were decomposed following Lorentz function fits in order to quantify the area corresponding to the diffraction peaks (110) and (200) and to the amorphous halo, as exemplified in Fig. 6(a) for the original LMDPE. Fig. 6(b) shows typical curves of X-ray scattering as a function of scattering angle obtained for LMDPE-BPO, LMDPE-AGE-1 and LMDPE-AGE-2. The diffraction peaks at 21.4 and 23.7° correspond to the diffraction planes (110) and (200) of all samples (Table 3) [35].

The distance periodicity $d$ was determined by applying the Bragg equation:

$$d = \frac{2\sin\theta}{\lambda} \tag{12}$$

where $\theta$ is the half of the diffraction angle of the peak and $\lambda$ is the wavelength of the X-ray.

The characteristic lattice constants a and b determined from $d$ and the Miller indices amounted to 0.74 and 0.49 nm, respectively. These values are identical with those reported for poly(ethylene) [34], indicating that LMDPE, LMDPE-BPO, LMDPE-AGE-1 and LMDPE-AGE-2 belong to the orthorhombic crystal class. The determination of c constant would require small angle X-ray scattering measurements.

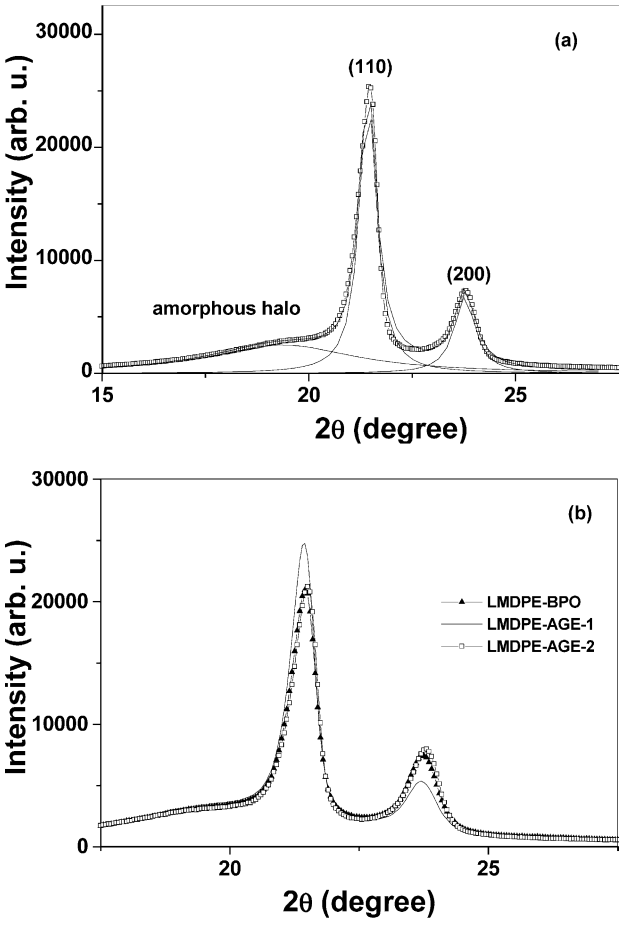


Fig. 6. (a) Typical X-ray scattering as a function of scattering angle obtained for LMDPE with curve decomposition following Lorentz function fits. (b) X-ray scattering as a function of scattering angle obtained for LMDPE-BPO, LMDPE-AGE-1 and LMDPE-AGE-2.

The diffractograms in Fig. 6 are characterized by the presence of an amorphous halo and two diffraction peaks. In order to compare the relative areas corresponding to the amorphous and the crystalline region, the percentage corresponding to each peak area in relation to the sum of all areas was calculated for each sample (percentages in the brackets in Table 3). The amorphous region in original LMDPE samples corresponded to 40% of total area. After

Table 3
Areas corresponding to the diffraction peaks (110) and (200) and to the amorphous halo and peak positions for LMDPE, LMDPE-BPO, LMDPE-AGE-1 and LMDPE-AGE-2

| Sample | Area, (110) (a.u.) | Area, (200) (a.u.) | Area, amorphous halo (a.u.) | Peak, position (110) (degree) | Peak, position (200) (degree) |
|---|---|---|---|---|---|
| LMDPE | 19322, (45%) | 6543, (15%) | 17026, (40%) | 21.4 | 23.7 |
| LMDPE-BPO | 16927, (38.5%) | 7178, (16.5%) | 19836, (45%) | 21.4 | 23.7 |
| LMDPE-AGE-1 | 19375, (43%) | 5031, (11%) | 20823, (46%) | 21.4 | 23.7 |
| LMDPE-AGE-2 | 16952, (39%) | 7435, (17%) | 19346, (44%) | 21.4 | 23.8 |

The area values are resulting from decompositions following Lorentz fits. The figures in the brackets represent the percentage corresponding to each peak area in relation to the sum of all areas.

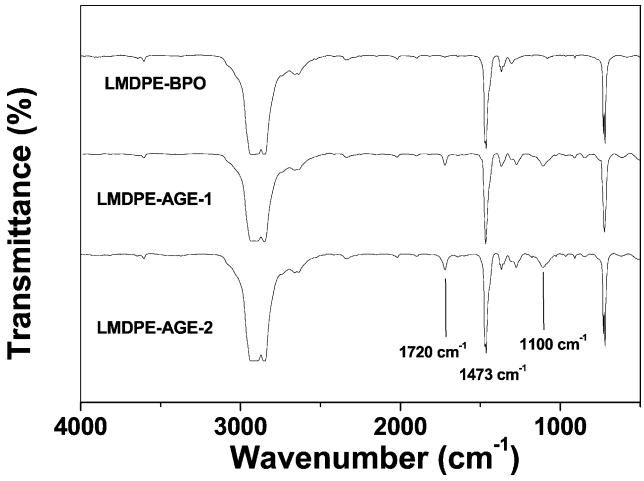


Fig. 7. FTIR spectra obtained for LMDPE-BPO, LMDPE-AGE-1 and LMDPE-AGE-2 samples just after processing.

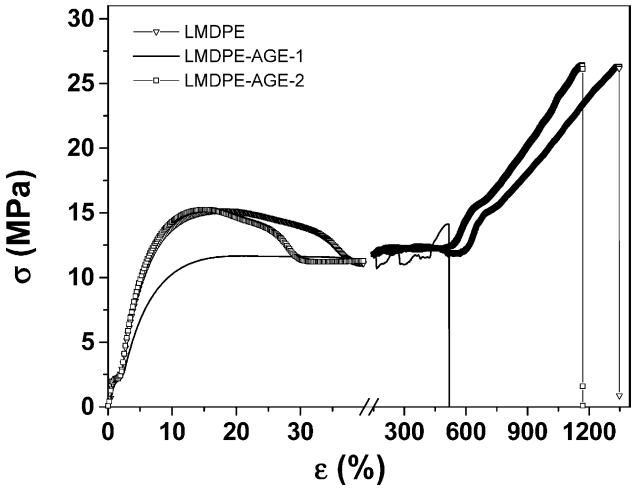


Fig. 8. Stress–strain curves obtained for LMDPE, LMDPE-AGE-1 and LMDPE-AGE-2.

processing in the presence of BPO, the amorphous region in LMDPE-BPO samples corresponded to 45% of total area. Grafting AGE onto the LMDPE samples led amorphous regions of 44 and 46% of total area. This finding shows that processing LMDPE with BPO alone is enough to increase the amorphous region. The areas corresponding to the (110) diffraction peak presented a small decrease after processing in the presence of BPO or BPO and AGE. In the case of LMDPE-AGE-1 the area corresponding to the (200) peak decreased in relation that calculated for the original LMDPE samples. In contrast, for samples LMDPE-BPO and LMDPE-AGE-2 the area corresponding to the (200) peak presented a small area increase in relation to that calculated for the original LMDPE samples. One should be aware that these calculations are resulting from Lorentz function fits and should be taken as indicative for a tendency. The tendencies here show that after processing LMDPE samples in the presence of BPO or BPO and AGE the amorphous halo areas increase $(5\pm1)\%$ in comparison to LMDPE samples. This finding indicates that the decrease in the polymer crystallinity is due to processing and functionalization. Nevertheless, the lattice constants have not been affected by the processing nor by the functionalization, since no change in the (110) and (200) peaks positions could be observed.

The purification of the functionalized samples described in the experimental part is very important to determine the amount of AGE chemically bound to the polyolefin. However, for practical purposes, the composites are prepared with functionalized samples as they come out of the mixer. Fig. 7 shows the FTIR spectra obtained for LMDPE-BPO, LMDPE-AGE-1 and LMDPE-AGE-2, just after processing. A carbonyl characteristic band at 1720 $cm^{-1}$ is present in the spectra obtained for LMDPE-AGE-1 and LMDPE-AGE-2, but absent in the spectrum obtained for LMDPE-BPO, indicating that processing BPO and AGE together without mixer degassing might favor oxidative process.

### 3.2. Composites of LMDPE-AGE and cellulose

Stress–strain curves obtained for LMDPE, LMDPE-AGE-1 and LMDPE-AGE-2 are shown in Fig. 8. The tensile behavior observed for LMDPE samples was similar to that observed for LMDPE-BPO samples (stress–strain curve not shown). The tensile properties are presented in Table 4. The mechanical performance observed for LMDPE-AGE-1 samples is the poorest, confirming that grafting AGE onto LMDPE with large amounts of BPO led not only to the to chain functionalization, but also chain scission, as evidenced by the low $\tau_f$ values (Fig. 3 and Table 1). Nevertheless, all samples presented ductile behavior with necking.

Table 4
Tensile properties determined for LMDPE, LMDPE-BPO, LMDPE-AGE-1 and LMDPE-AGE-2: stress at the yield point ($\sigma_Y$), elongation at the yield point ($\varepsilon_Y$), maximum stress ($\sigma_M$), fracture stress ($\sigma_b$), fracture elongation ($\varepsilon_b$) and Young's modulus ($E$)

| Sample | $\sigma_Y$ (MPa) | $\varepsilon_Y$ (%) | $\sigma_M$ (MPa) | $\sigma_b$ (MPa) | $\varepsilon_b$ (%) | E (GPa) |
|---|---|---|---|---|---|---|
| LMDPE[a] | 15.1±0.3 | 18.6±0.8 | 26.6±0.7 | 26.2±0.6 | 1361±33 | 0.26±0.02 |
| LMDPE-BPO[a] | 13.0±0.2 | 16.6±0.2 | 26.6±0.8 | 26.1±0.8 | 1190±35 | 0.16±0.05 |
| LMDPE-AGE-1 | 11.3±0.4 | 27±16 | 14±2 | 14±1 | 519±161 | 0.10±0.03 |
| LMDPE-AGE-2 | 15.2±0.1 | 15.1±0.3 | 26.4±0.4 | 26.1±0.2 | 1174±23 | 0.33±0.03 |

The figures represent mean values of five replicates.
[a] Processed during 10 min at 60 rpm at 120 °C.

Table 5
Tensile properties determined for composites prepared with short cellulose (SC) fibers: stress at the yield point ($\sigma_Y$), elongation at the yield point ($\varepsilon_Y$), maximum stress ($\sigma_M$), fracture stress ($\sigma_b$), fracture elongation ($\varepsilon_b$) and Young's modulus ($E$)

| | SC (wt%) | $\sigma_Y$ (MPa) | $\varepsilon_Y$ (%) | $\sigma_M$ (MPa) | $\sigma_b$ (MPa) | $\varepsilon_b$ (%) | E (GPa) |
|---|---|---|---|---|---|---|---|
| LMDPE-SC20 | 20 | 18.7±0.8 | 4.3±0.1 | 20.6±0.5 | 18±1 | 13.6±0.9 | 0.64±0.02 |
| LMDPE-AGE-1-SC20 | | 13.9±0.7 | 5.4±0.3 | 14.9±0.4 | 10.5±0.7 | 24±3 | 0.40±0.03 |
| LMDPE-AGE-2-SC20 | | 16.0±0.5 | 5.2±0.2 | 19.1±0.5 | 14±2 | 27±3 | 0.52±0.02 |
| LMDPE-SC30 | 30 | 19.2±0.5 | 5.3±0.6 | 20.3±0.7 | 14±1 | 30±1 | 0.55±0.02 |
| LMDPE-AGE-1-SC30 | | 16.7±0.7 | 4.6±0.2 | 21±1 | 19±1 | 20±3 | 0.58±0.06 |
| LMDPE-AGE-2-SC30 | | 20.9±0.4 | 5.5±0.3 | 23.2±0.3 | 21.7±0.3 | 27±3 | 0.71±0.02 |
| LMDPE-SC40 | 40 | 14.6±0.8 | 3.2±0.3 | 16.9±0.7 | 12.0±0.9 | 6.0±0.6 | 0.84±0.03 |
| LMDPE-AGE-1-SC40 | | 18±1 | 4.1±0.2 | 20.3±0.6 | 20.0±0.5 | 10±2 | 0.69±0.02 |
| LMDPE-AGE-2-SC40 | | 25.3±0.7 | 4.5±0.1 | 29.4±0.4 | 28±1 | 17±1 | 1.01±0.05 |
| LMDPE-SC50 | 50 | 7.6±0.3 | 2.62±0.02 | 7.7±0.4 | 4±1 | 5.0±0.4 | 0.50±0.04 |
| LMDPE-AGE-1-SC50 | | 22±1 | 3.82±0.02 | 24.7±0.9 | 24.6±0.9 | 8.1±0.7 | 0.96±0.03 |
| LMDPE-AGE-2-SC50 | | 24.5±0.5 | 4.0±0.3 | 27.4±0.6 | 27.2±0.6 | 12.0±0.9 | 1.02±0.04 |

The figures represent mean values of five replicates.

Comparing typical stress–strain curves obtained for composites shown in Fig. 9 with those obtained for the polymeric matrix (Fig. 8) two effects can be observed: upon the addition of cellulose fibers the modulus ($E$) values increased and the elongation decreased. In order to evaluate the compatibilizing effect of AGE on the composites performance, control composites of LMDPE and SC in the absence of AGE and BPO were prepared at the same conditions and their tensile properties were measured. Moreover, the effect of filler content on the composites tensile properties was investigated for composites with short cellulose fibers, as presented in Table 5. Some remarks can be made with basis on the data presented in Table 5.

The compatibilizing effect of AGE on the composites mechanical performance was more pronounced when LMDPE-AGE-2, instead of LMDPE-AGE-1, was used in the formulation. This is explained by the poor tensile properties of LMDPE-AGE-1, as already discussed. However, the LMDPE-AGE-1-SC, regardless the filler content, showed higher values of E, $\sigma_M$, and $\sigma_b$ in relation to those values found for LMDPE-AGE-1. Similar results were also observed for composites of maleated polyethylene and cellulose [36].

Comparing the effect of SC content on the composites prepared with LMDPE and LMDPE-AGE-2, one can observe that the compatibilizing effect becomes significant when the filler content is 30 wt% or higher than this. Similar effects have been observed for natural fiber composites [6,37–39]. Fig. 10 shows this effect on the $E$ and $\sigma_M$ values obtained for composites prepared with original LMDPE and

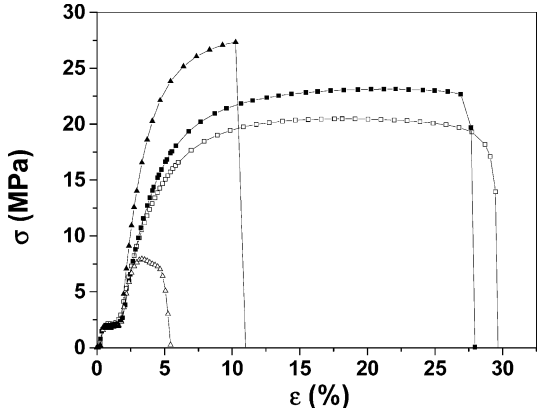


Fig. 9. Stress–strain curves obtained for the composites LMDPE-SC30 (open squares), LMDPE-AGE-2-SC30 (solid squares), LMDPE-SC50 (open triangles), LMDPE-AGE-2-SC50 (solid triangles).

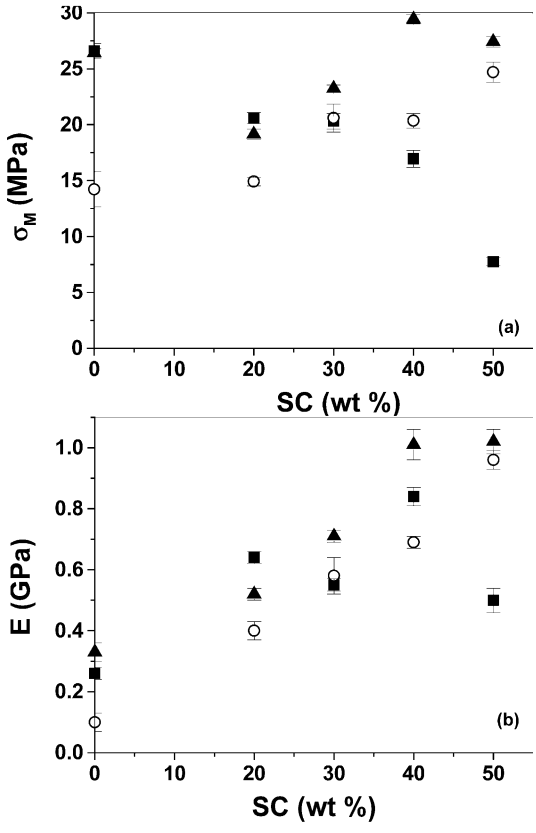


Fig. 10. The effect of cellulose fiber content on the $\sigma_M$ (a) and $E$ (b) values for LMDPE (solid squares), LMDPE-AGE-1 (open circles) and LMDPE-AGE-2 (solid triangles) samples.

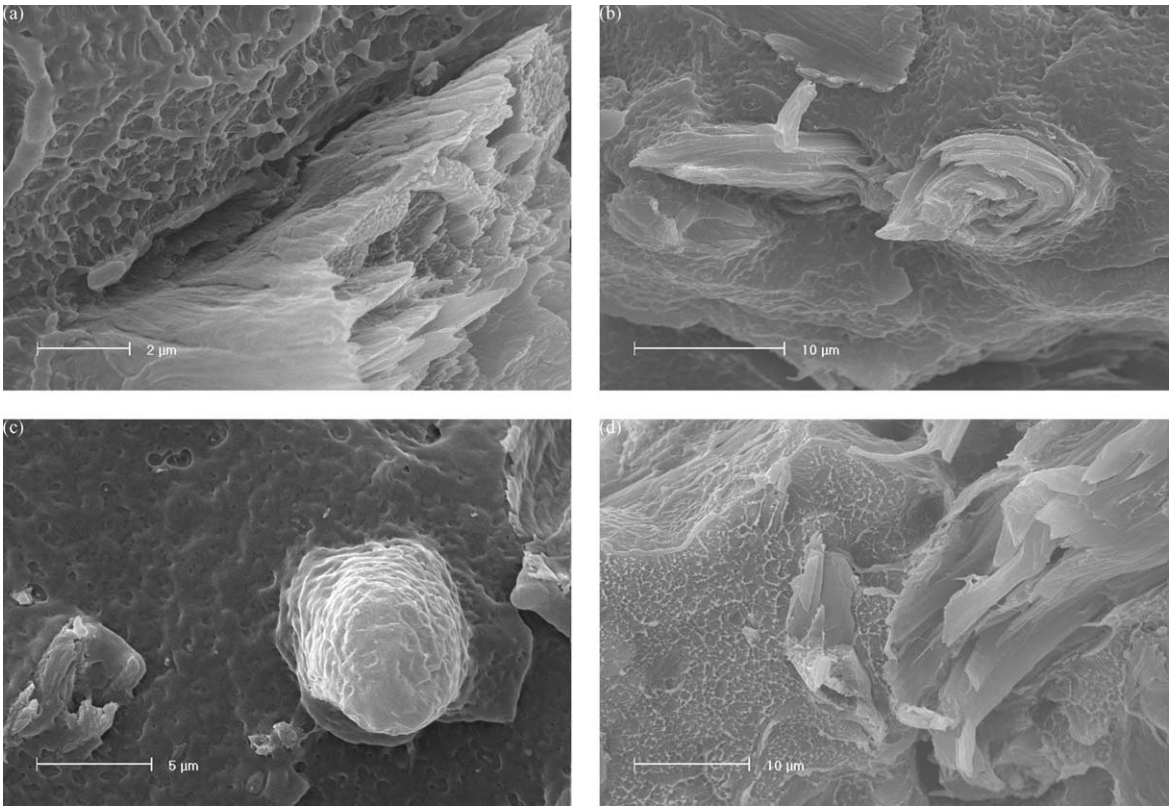


Fig. 11. Scanning electron micrographies of crio-fracture surfaces of (a) LMDPE-SC30 (bar = 2 μm), (b) LMDPE-AGE-2-SC30 (bar = 10 μm), (c) LMDPE-AGE-2-SC40 (bar = 5 μm) and (d) LMDPE-AGE-2-SC50 (bar = 10 μm).

AGE functionalized LMDPE samples. This is a very interesting result because it shows that although the degree of functionalization is low, the small amount of AGE groups attached to the LMDPE chains is enough to improve the interfacial adhesion between cellulose and polymeric matrix. One can expect a chemical reaction between the cellulose hydroxyl groups and the LMDPE-AGE epoxy groups by a SN2 mechanism, which is a typical reaction for epoxy groups [40]. Besides the chemical binding, strong physical binding as H bonding is also expected.

### *3.3. Scanning electron microscopy on the composites*

SEM images obtained for the composites LMDPE-SC30, LMDPE-AGE-2-SC30, LMDPE-AGE-2-SC40 and LMDPE-AGE-2-SC50 are shown in Fig. 11(a), (b), (c) and (d), respectively. Fig. 11(a) shows a disconnected interface with voids between LMDPE and fiber. In contrast, in the fracture surface of composites made up of AGE functionalized LMDPE and fibers (Fig. 11(b)–(d)) the fibers appear embedded in the polymeric matrix. Fig. 11(b) presents interesting features, one can see a fiber in the left side, which is not completely adhered to the matrix, but the fiber in the right side seems to be tightly bound to the polymer. This might be explained with basis on the distribution of AGE grafted onto the polymer, which is probably heterogeneous because of the low degree of functionalization. These SEM images show that, although the amount of grafted AGE onto LMDPE is low, AGE plays an important role in the interfacial adhesion between the functionalized LMDPE-AGE and SC fibers.

## 4. Conclusions

AGE forms unstable and energetically rich macroradicals. It has been successfully grafted onto LMDPE chains in an internal laboratory mixer in the presence of BPO. Upon increasing the BPO content in the mixture, grafting and chain scission were favored. Low amount of BPO led to low degree of functionalization and no measurable chain scission. AGE functionalized LMDPE presented lower crystallinity than original LMDPE chains. The tensile performance of composites prepared with AGE functionalized LMDPE and cellulose fibers was superior to that observed for composites of unmodified LMDPE and cellulose when the filler content was higher than 30 wt%. These findings show that although the degree of AGE functionalization onto LMDPE is lower than 1 wt% of AGE, good interfacial adhesion with cellulose fibers has been achieved.

## Acknowledgements

The authors are grateful to FAPESP, CAPES and CNPq for financial support, to Eng. Sérgio D. Almeida (Politeno, SP) for supplying the polyolefin samples and to Caio Dimisson for technical support.

## References

[1] Bledzki AK, Gassan J. J Prog Polym Sci 1999;24:221–74.
[2] Castellano M, Gandini A, Fabbri P, Belgacem MN. J Colloid Interf Sci 2004;273:505–511.
[3] Zhang F, Qiu W, Yang L, Endo T, Hirotsu T. J Appl Polym Sci 2003; 89:3292–9.
[4] Zhang F, Endo T, Qiu W, Yang L, Hirotsu T. J Appl Polym Sci 2002; 84:1971–9.
[5] Li Q, Matuana LM. J Appl Polym Sci 2003;88:278–84.
[6] Marcovich NE, Villar MA. J Appl Polym Sci 2003;90:2775–84.
[7] Hedenberg P, Gatenholm P. J Appl Polym Sci 1995;56:641–8.
[8] Felix JM, Gatenholm P. J Appl Polym Sci 1991;42:609–16.
[9] Karani R, Krishnan M, Narayan R. Polym Eng Sci 1997;37:476–83.
[10] Yang CQ. J Appl Polym Sci 1993;50:2047–54.
[11] Moad G. Prog Polym Sci 1999;24:81–142.
[12] Campos PGS, Fantini MCA, Petri DFS. J Braz Chem Soc 2004;15: 532–40.
[13] Liu NC, Xie HQ, Baker WE. Polymer 1993;34:4680–7.
[14] Papke N, Karger-Kocsis J. J Appl Polym Sci 1999;74:2616–24.
[15] Torres N, Robin JJ, Boutevin B. J Appl Polym Sci 2001;81:581–90.
[16] Tarducci C, Kinmond EJ, Badyal JPS. Chem Mater 2000;12:1884–9.
[17] Sun Y-J, Hu G-H, Lambla M. J Appl Polym Sci 1995;57:1043–54.
[18] Kim C-H, Cho KY, Park J-K. Polymer 2001;42:5135–42.
[19] Cartier H, Hu G-H. J Polym Sci, Part A: Polym Chem 1998;36: 2763–74.
[20] Pesetskii SS, Jurkowski B, Makarenko OA. J Appl Polym Sci 2002; 86:64–72.
[21] Sebe G, Brook MA. Wood Sci Technol 2001;35:269–76.
[22] Petri DFS, Choi SW, Beyer H, Schimmel Th, Bruns M, Wenz G. Polymer 1999;40:1593–601.
[23] Timar MC, Pitman MC, Mihai MD. Int Biodeterior Biodegrad 1999; 43:181–8.
[24] Solpan D, Guven O. Angew Makromol Chem 1999;269:30–4.
[25] Cetin NS, Hill CAS. J Wood Chem Technol 1999;19:247–52.
[26] Burton SC, Harding DRK. J Chromatogr A 1997;775:39–46.
[27] Sclavons M, Franquinet P, Carlier V, Verfaillie G, Fallais I, Legras R, et al. Polymer 2000;41:1989–99.
[28] Bettini SHP, Agnelli JAM. J Appl Polym Sci 1999;74:247–55.
[29] Gaylord NG, Mehta R, Kumar V, Tayi M. J Appl Polym Sci 1989;38: 359–71.
[30] Sun Y-J, Hu GH, Lambla M. Angew Makromol Chem 1995;229: 1–13.
[31] Ham GE. J Macromol Sci Chem 1975;A9(4):635–6.
[32] Vollmert B. Grundriss der Makromolecularen Chemie. Band I. Karlsruhe, Germany: Verlagsdruckerei; 1988. 154–160.
[33] Wunderlich B, Cormier CM. J Polym Sci 1967;A-2(5):987–90.
[34] Elias HG. An introduction to polymer science. 1st ed 1997. New York: VCH Verlagsgesellschaft mbH.
[35] Androsch R. Polymer 2000;40:2805–12.
[36] Zhang F, Endo T, Qiu W, Yang L, Hirotsu T. J Appl Polym Sci 2002; 84:1971–80.
[37] Jana SC, Prieto A. J Appl Polym Sci 2002;86:2159–67.
[38] Rarjeev K, Krishanan M, Narayan R. Polym Eng Sci 1997;37:476–83.
[39] Qiu W, Zhang F, Endo T, Hirotsu T. J Appl Polym Sci 2002;87: 337–45.
[40] March J. Advanced organic chemistry: reactions, mechanisms, and structure. 3rd ed. New York: Wiley; 1985. p. 346.